Applied Catalysis B: Environmental 179 (2015) 542–550

Contents lists available at ScienceDirect

Applied Catalysis B: Environmental

journal homepage: www.elsevier.com/locate/apcatb

Evaluation of H_2 effect on NO oxidation over a diesel oxidation catalyst

Muhammad Mufti Azis, Xavier Auvray[1], Louise Olsson, Derek Creaser*

Competence Center for Catalysis, Department of Chemistry and Chemical Engineering, Chalmers University of Technology, SE-412 96 Göteborg, Sweden

ARTICLE INFO

Article history:
Received 4 March 2015
Received in revised form 20 May 2015
Accepted 29 May 2015
Available online 1 June 2015

Keywords:
Hydrogen
Diesel oxidation catalyst
NO oxidation
Pt oxide
Exhaust emission

ABSTRACT

The influence of H_2 on NO oxidation over Pt/Al_2O_3 as a model DOC catalyst was evaluated with various DOC feed mixtures. Discrimination of surface chemistry and exothermal effects due to addition of H_2 was made based on differences in time scales of transient responses. H_2 was proposed to retard Pt oxide formation mainly at low temperatures (ca. <200 °C), whereas, at higher temperatures Pt oxide formation was unhindered by H_2. As a result, a temporal enhancement in NO_2 yield due to H_2 was obtained during temperature ramp experiments. In C_3H_6 containing mixtures, it was evident that the promotional role of H_2 was to weaken the inhibition effect of C_3H_6 by lowering the light-off temperature for C_3H_6 oxidation. The results from transient experiments clearly showed an increase in NO_2 yield that resulted from effects of H_2 on surface chemistry and/or reactions. H_2 decreased the blocking effect of adsorbed C_3H_6 species and prevented the reaction of C_3H_6 with NO_2 forming NO. For a complete DOC feed mixture (containing NO, CO, C_3H_6), an addition of ca. 250 ppm of H_2 appeared to be optimal, while higher H_2 concentrations were disadvantageous due to NO_2 consumption by H_2.

1. Introduction

In light of the concern to reduce fuel consumption and global warming, emission aftertreatment for lean-burn gasoline and diesel engines has been gaining more attention than that for conventional stoichiometric gasoline engines. With an ample O_2 concentration in the lean-burn or diesel exhaust, the use of conventional three-way catalysts is not effective to lower NO_x emissions to environmentally acceptable levels. Thus, a more complex catalytic aftertreatment system that primarily consists of a diesel oxidation catalyst (DOC), diesel particulate filter (DPF) and a selective catalytic reduction (SCR) catalyst are commonly employed.

The DOC, as a part of a diesel aftertreatment system, has the duty to oxidize CO and hydrocarbons (HC). In addition, the DOC facilitates oxidation of NO–NO_2 which is advantageous for soot and NO_x removal by the downstream DPF and SCR units [1]. With its oxidative power, NO_2 enhances combustion of trapped particulate matter in the DPF. This passive regeneration of the DPF allows for lower fuel penalties compared to active regeneration processes. The presence of NO_2 in the exhaust also accelerates the selective catalytic reduction of NO_x by NH_3 (supplied in the form of urea) which is the most common currently applied NO_x removal process for mobile applications.

Alumina-supported platinum catalysts are common and efficient catalysts for oxidation reactions, including NO oxidation. Oxidation of NO to NO_2 with O_2 excess is known to be restricted by thermodynamics at high temperature [2]. Although they display high NO oxidation activity, the produced NO_2 has been shown to self-inhibit the NO oxidation [3,4]. Olsson and Fridell [5] as well as Bhatia et al.[4] have shown that formation of Pt oxide is responsible for the activity drop of NO oxidation as a function of time over Pt/Al_2O_3. This can be attributed to the oxygen-rich operating conditions [6] and the strong oxidative power of NO_2 [5]. With respect to this, Pt oxide formation has been suggested to explain activity hysteresis behavior during temperature ramp experiments [6–9]. During an NO oxidation test run, the conversion measured during the cooling ramp is typically lower than the preceding heating ramp. Further, reversible Pt oxidation by NO_2 as well as reduction of Pt oxide by NO have also been suggested as the reactions leading to hysteresis [8].

Herreros et al.[10] recently reported on the promoting effect of H_2 addition in real diesel exhausts on the oxidation activity of Pt and Pt-Pd DOC catalysts. They observed an improvement in NO_2 formation in addition to HC and CO conversion. Only a portion of this promotional effect was found to stem from the temperature rise due to H_2 oxidation. The intrinsic contribution of H_2 is however difficult to determine due to the complex gas composition of real diesel exhaust. Related to the catalyst deactivation by Pt oxidation

* Corresponding author. Tel.: +46 31 772 3023; fax: +46 31 7723035.
E-mail address: derek.creaser@chalmers.se (D. Creaser).
[1] Present address: Department of Chemical Engineering, Norwegian University of Science and Technology (NTNU), Trondheim, Norway.

http://dx.doi.org/10.1016/j.apcatb.2015.05.054
0926-3373/

as mentioned earlier, it is thus of interest to investigate if addition of a particularly reactive reductant like H_2 may influence Pt oxide formation. In addition, cofeeding of H_2 into the lean gas mixture may also lead to NO_x reduction to N_2O and N_2 over Pt catalysts. This process is known as H_2-SCR and has been widely investigated in the literature, interested readers can read a review of this method e.g., in [11]. For other catalytic systems such as Ag/Al_2O_3, it is already well documented that H_2 promotes oxidation of NO to NO_2 as well as SCR activities with HC or NH_3 reductants [12].

The promotional effect of H_2 on exclusively low temperature CO oxidation over Pt/Al_2O_3 catalysts has been more widely studied [13–15]. It has been proposed to result from interactions between surface species causing a reduction in CO desorption activation energy [4,16] or coupling of the CO and H_2 oxidation surface chemistries via the hydroxyl intermediate [17–19]. These mechanisms that enhance CO oxidation may also be linked to the improved NO oxidation.

The presence of HC in exhaust, derived from unconverted fuel and lubricating oil, is common. For a DOC, admission of C_3H_6 (as a HC model compound) has been found to inhibit NO oxidation and vice versa [20–23]. Conversely, H_2 reportedly promotes the oxidation performance of Pt/Al_2O_3 [10]. It is thus of interest to investigate the interplay between the inhibition effect of C_3H_6 and promotion effect of H_2 on the NO oxidation reaction. Using Pt/Al_2O_3, addition of C_3H_6 to a gas containing NO_x may also lead to its conversion to N_2O and N_2 via the HC-SCR process and addition of H_2 has also been reported to boost its low temperature activity [24].

The aim of the present work was to evaluate the effect of H_2 on the NO oxidation reaction over Pt/Al_2O_3. Of interest are to what extent the mechanisms mentioned above or others may promote specifically NO oxidation over Pt/Al_2O_3 under varying lean diesel exhaust feed conditions and temperatures. The effect of CO and C_3H_6 in the inlet feed, combined with different concentrations of H_2, was investigated systematically. In addition, transient experiments with H_2 switched in and out of the feed were also conducted to identify the time scale of the H_2 effect with various gas mixtures. Finally the surface chemistry and exothermal heat effect due to H_2 addition were quantitatively discriminated.

2. Experimental methods

2.1. Catalyst preparation

The catalyst powder containing 1 wt.% Pt was prepared by wet impregnation. A slurry consisting of pre-calcined γ-alumina (Puralox SBa-200, Sasol, 2.5 h at 750 °C) and purified deionized "MilliQ" water (Millipore) was maintained under stirring while the pH was monitored. A ratio of 16 mL water per gram of alumina was used. Nitric acid was then added drop-wise to reach a stable pH of ca. 4. A solution containing the Pt was prepared by dilution of the appropriate amount of $Pt(NO_3)_2$ (Heraeus) in 40 mL MilliQ water. It was then added drop-wise to the stirred alumina slurry. During this operation, the pH decreased. After ca. 2 h under stirring, the solution was frozen by dipping in liquid N_2 and dried overnight under vacuum so as to sublimate the water. The resulting catalyst powder was calcined in air at 500 °C for two hours.

2.2. Monolith preparation

The catalyst studied was washcoated onto a honeycomb-structured cordierite monolith by dipping a pre-calcined (2 h at 600 °C in air) monolith in a catalyst powder suspension. The monolith was 2 cm long and had a 2 cm diameter and a channel density of 400 cpsi. The catalyst powder was mixed with a binder (boehmite Disperal P2, Sasol, 80 wt.% catalyst/20 wt.% binder) and dispersed in a solution made of 50 wt.% ethanol and 50 wt.% water. The liquid-to-solid mass ratio of the slurry was around 7 to ensure the deposition of a significant amount of washcoat in each dipping and at the same time avoid channel clogging. After each dipping, the monolithic sample was dried with a hot air gun at ca. 90 °C until evaporation of the liquid. During this step, the sample was continuously flipped with care to ensure the homogeneous distribution in the channels. Drying at 550 °C was then performed for one minute. The dipping and drying process was repeated until ca. 0.5 g washcoat was deposited. The monoliths were then calcined in a furnace at 550 °C in air for two hours.

2.3. Flow reactor experiment

Activity measurements were conducted on a flow reactor with synthetic gas mixtures. The monolith sample was placed in a hollow horizontal quartz tube equipped with an electric heating coil. All gas lines before and after the reactor were heated accordingly to avoid water condensation. Two thermocouples (type K) were installed; one was placed inside the sample ca. 0.5 cm from the outlet end of monolith to indicate the monolith or catalyst temperature and the other thermocouple was inserted through the monolith from the outlet end and protruded ca. 1 cm from the inlet part of the sample to indicate the gas inlet temperature.

The inlet gases were supplied by a number of separate mass flow controllers, whereas water vapor was provided by a controlled evaporation and mixing system (all Bronkhorst Hi-Tech). The outlet gases were analyzed continuously by gas FTIR (MKS 2000) and a small portion of the outlet flow was also analyzed by Mass Spectrometry (Hiden Quadruple). Gas FTIR was the primary gas analysis method and used to measure NO, NO_2, N_2O and NH_3 in ppm levels. In addition, H_2O was monitored by FTIR in percentage levels. Mass Spectrometry was mainly used to monitor H_2 from the m/e 2 signal.

The N balance was evaluated according to:

$$N\text{balance}(\%) = \frac{(NO + NO_2 + 2 \cdot N_2O + NH_3)_{outlet}}{NO_{inlet}} \times 100 \quad (1)$$

From Eq. (1), it can be seen that *N* balance values lower than 100% indicate either the conversion of NO_x to N_2 or the storage of NO_x on the catalyst.

2.4. Temperature-programmed reaction (TPR) experiments

The washcoated monolith used in the present study was used in a previous study [25] where it was seen to have stable activity for NO oxidation even after several pretreatment cycles. Prior to each experiment in the present work, the catalyst was pretreated consecutively under the following oxidative and reductive dry atmospheres with total flows of 1000 mln/min at 450 °C:

- 10% O_2 in Ar (balance in all experiments) with duration of 20 min.
- 2% H_2 in Ar with duration of 30 min.

The above pretreatment step was intended to obtain a Pt oxide free surface over the catalyst. Following pretreatment, the reactor temperature was then decreased to 120 °C in Ar flow. TPR experiments were carried out by heating up the reactor to 500 °C with a ramping rate of 5 °C/min. After holding the temperature at 500 °C for 5 min, the reactor temperature was then cooled down to 120 °C with the same rate of 5 °C/min. A total flow of 3000 mL n/min (corresponds to Weight Hourly Space Velocity, WHSV, of 562 h^{-1} or equivalent to Gas Hourly Space Velocity, GHSV, of ca. 29000 h^{-1}) was used in all experiments except the pretreatment conditions. Table 1 displays the gas mixture inlet compositions used in the TPR experiments.

Table 1
Inlet gas mixtures used in present work.

Gas mixture notation	Inlet composition
NO/O_2	500 ppm NO, 8% O_2, 5% H_2O and varied H_2 (0, 250, 500, 750, 1000 ppm).
$NO/O_2/CO$	500 ppm NO, 8% O_2, 200 ppm CO, 5% H_2O and varied H_2 (0, 250, 500, 750, 1000 ppm).
$NO/O_2/C_3H_6$	500 ppm NO, 8% O_2, 200 ppm C_3H_6, 5% H_2O and varied H_2 (0, 250, 500, 750, 1000 ppm).
$NO/O_2/CO/C_3H_6$	500 ppm NO, 8% O_2, 200 ppm C_3H_6, 200 ppm CO, 5% H_2O and varied H_2 (0, 250, 500, 750, 1000 ppm).

2.5. Transient experiments

In transient experimental mode 1, the role of H_2 to influence the NO_2 yield at a certain temperature was investigated. For this purpose, following catalyst pretreatment at 450 °C, the catalyst temperature was decreased to 120 °C. Subsequently, the catalyst temperature was raised to 230 °C with a heating rate of 5 °C/min with a NO/O_2 mixture or cofeeding of constant H_2 concentration of 750 ppm with each of the following mixtures: NO/O_2, $NO/O_2/C_3H_6$ and $NO/O_2/CO/C_3H_6$ as previously tabulated in Table 1. At 230 °C, the gas temperature was held constant for 1 h with the corresponding gas mixture.

In transient experimental mode 2, the dynamic effect of H_2 was investigated by exposing the catalyst intermittently to H_2. In this transient test, again, only 750 ppm H_2 was fed with each gas mixture in Table 1. The same procedure of pretreatment and heating to 230 °C in the presence of H_2 was conducted as in transient experimental mode 1. The gas temperature was then held constant at 230 °C and 750 ppm of H_2 feed was switched in and out with 10 min duration for each pulse.

3. Results

3.1. The effect of H_2 with various gas mixtures

Fig. 1 shows the results of the H_2 effect on NO oxidation as a function of catalyst temperature with various gas mixtures, during TPR heating ramps that were preceded by catalyst pretreatment and inert cooling steps. When NO_2 yield is not limited by equilibrium, it is possible that NO_2 yield can be improved simply due to the increase of catalyst temperature resulting from H_2 combustion. Here, the results are plotted against the measured catalyst temperature instead of the inlet temperature. As a result any observed increased yields of NO_2 should not be related to the exothermal reaction heat. The "catalyst temperature" here is a measure of the temperature near the outlet end of the monolith. The monolith reactor used was not entirely isothermal nor adiabatic. At high operating temperature, exceeding about 350 °C heat loss from the reactor was significant and resulted in lower measured catalyst temperature. However, at lower operating temperatures when NO oxidation was kinetically controlled, this heat loss was minor and the reaction exotherms typically resulted in catalyst temperatures exceeding the inlet temperatures. H_2 combustion could result in an axial temperature gradient over the monolith where higher H_2 feed concentration causes increasingly higher outlet temperatures. For H_2 oxidation at 230 °C, the adiabatic temperature increase is 11 °C from complete conversion of 1000 ppm of H_2. The comparisons here based on measured catalyst temperature instead of inlet temperature should in fact provide a modest estimate of any promotional effects of H_2 minus exothermal heat effects.

It should be noted that in general the effect of H_2 on the NO_2 yield varied, depending upon the temperature region and feed H_2 concentration. From observation of the H_2 signal (not shown), it

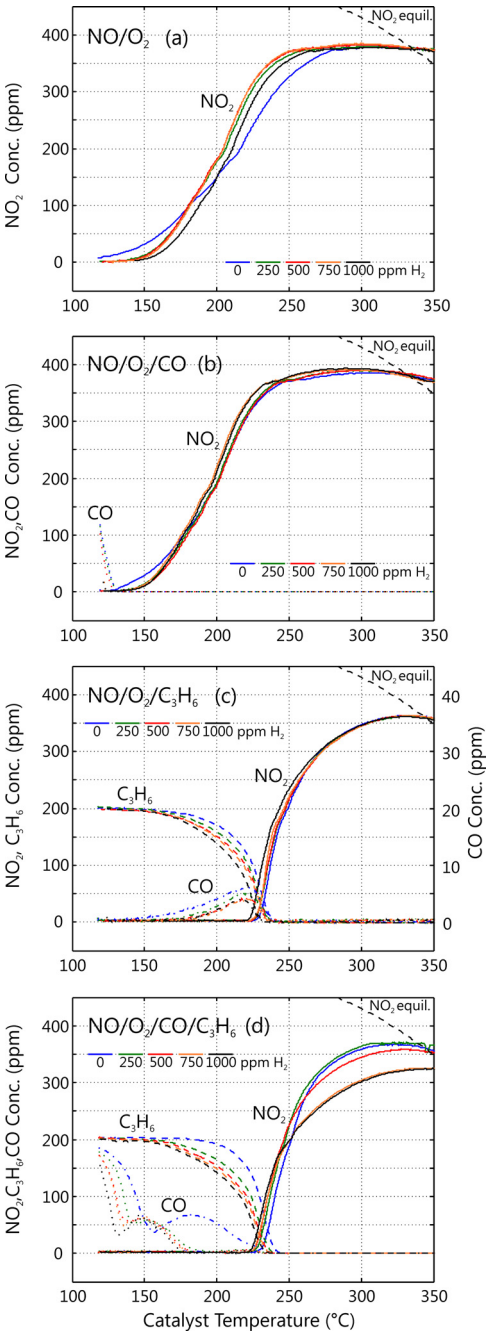

Fig. 1. The effect of H_2 concentration on NO oxidation over Pt/Al_2O_3 with various gas mixtures during heating ramp following pretreatment of the catalyst. See Table 1 for inlet feed condition.

was found that H_2 was generally already fully converted by 200 °C in all cases, even with the highest addition of 1000 ppm of H_2.

At temperatures exceeding about 300 °C, the NO_2 yield should be limited by thermodynamic equilibrium [2]. The equilibrium yield of NO_2 at the catalyst temperatures are indicated in Fig. 1 for each feed mixture. The onset of equilibrium limitation is evident in Fig. 1 for all gas mixtures by the leveling off and even eventual decreases in NO_2 yields at temperatures above 300 °C.

For the NO/O_2 mixture (Fig. 1a), it can be seen that addition of H_2 had both negative and positive effects on NO_2 yield. At low temperature (below 200 °C), addition of H_2 lowered the NO_2 yield. However, between 200 and 300 °C, H_2 was found to enhance NO_2 yield in this mixture. Concerning the H_2 promotional effect, it was

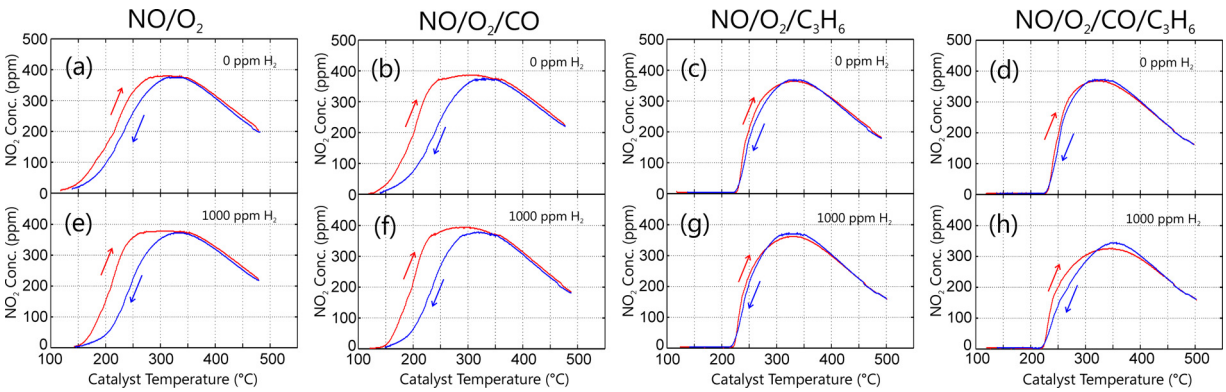

Fig. 2. The effect of H_2 on hysteresis behavior.

found that addition of H_2 up to 750 ppm improved NO_2 yield, however with 1000 ppm H_2 the NO_2 yield started to decrease.

From the $NO/O_2/CO$ gas mixture (Fig. 1b), it was observed that H_2 had little effect on the NO_2 yield, although a marginal increase in the NO_2 yield could still be seen between 180 and 300 °C with higher H_2 concentration. It is also worth noting that complete CO conversion in the absence of H_2 was attained already by ca. 135 °C. In the presence of H_2, the temperature for complete CO conversion was lowered to ca. 126 °C.

As shown in Fig. 1c for the $NO/O_2/C_3H_6$ mixture, a strong inhibition effect of C_3H_6 on NO oxidation was observed by the delayed light-off for NO oxidation to at least 220 °C. Addition of H_2 was however found to decrease the light-off temperature as well as to increase the NO_2 yield within temperature range of 220–325 °C. As the onset for C_3H_6 conversion started, there was also detectable formation of CO which was probably due to partial oxidation of C_3H_6.

Eventually, the effect of H_2 was also investigated on a complete mixture of $NO/O_2/CO/C_3H_6$ as displayed in Fig. 1d. The inhibition effect of C_3H_6 as well as the NO_2 light-off profile as in Fig. 1c was observed. Increasing the H_2 concentration was found to decrease the light-off temperature for NO, C_3H_6 and CO oxidation. Further, addition of 250 ppm H_2 was found to be beneficial for NO_2 yield in the temperature range above 220 °C. However, a further increase in H_2 concentration generally gave a lower NO_2 yield above 240 °C. The detrimental effect of H_2 was most prominent with H_2 concentrations of 750 and 1000 ppm. Inspection of the CO profile in Fig. 1d, indicates that addition of H_2 was also found to lower the temperature for complete CO conversion in this mixture. There was also a temporary increase in outlet CO as also previously observed in Fig. 1c, that was probably related to partial oxidation of C_3H_6.

3.2. The effect of H_2 on the hysteresis behavior

The hysteresis behavior of the NO oxidation reaction over Pt/Al_2O_3 is a well-known phenomenon [9]. Fig. 2 present the hysteresis loops for all mixtures as a function of catalyst temperature. By comparing the curves in the presence and absence of H_2, it is evident that addition of H_2 generally influenced the activity during both heating and cooling curves. To illustrate for the NO/O_2 mixture (Fig. 2a), the NO_2 yield during heating was always higher than that for the cooling process, as in agreement with literature. Addition of 1000 ppm of H_2 (Fig. 2e) gave a larger hysteresis loop than in the absence of H_2. For the $NO/O_2/CO$ gas mixture (2b and 2f), H_2 had nearly no effect on the size of the hysteresis loop.

The hysteresis loops for the C_3H_6 containing mixtures are presented in Fig 2c–d as well as g–h. Comparing Fig. 2a with 2c and 2d in the absence of H_2, it is evident that the hysteresis loop for the C_3H_6 containing mixtures was smaller than for the NO/O_2 mixture. Between 300–400 °C, the cooling curve was slightly higher than the heating curve. Addition of 1000 ppm of H_2 apparently amplified the superior activity during cooling as shown in Fig. 2g–h.

3.3. The effect of CO on NO and C_3H_6 oxidation in the absence of H_2

The base performance of the gas mixtures in the absence of H_2 during heating are compared in Fig. 3. As seen from Fig. 3a, CO had little influence on the light-off temperature for NO oxidation, but instead increased NO_2 yield only over a range of higher temperatures. The same also applied for NO_2 yield when adding CO

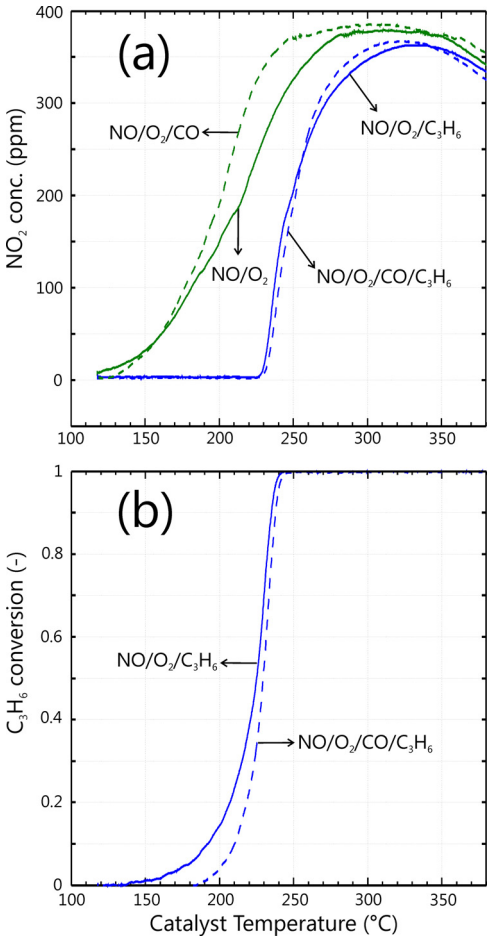

Fig. 3. Comparison of NO_2 yields (a) and C_3H_6 conversions (b) for gas mixtures without H_2.

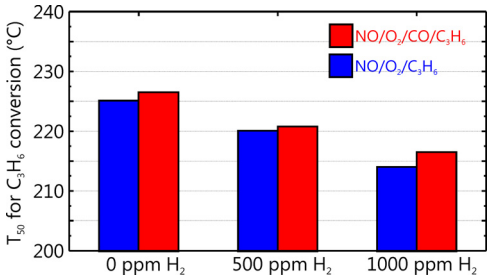

Fig. 4. The effect of H_2 on C_3H_6 light-off temperatures.

in C_3H_6 containing mixtures. Again, since the results are plotted against catalyst temperature the differences observed here should not result from the exothermal heat of CO or C_3H_6 combustion. Contrary to the enhancement effect of CO on NO_2 yield, the effect of CO on C_3H_6 conversion was slightly negative as it caused a higher light-off temperature for C_3H_6 conversion (Fig. 3b).

3.4. The effect of H_2 on light-off for C_3H_6 conversion

For the C_3H_6 containing gas mixtures, the effect of H_2 on the conversion of C_3H_6 is displayed in Fig. 4 based on T_{50}, the catalyst temperature required to reach 50% C_3H_6 conversion. Complete conversion of C_3H_6 was always eventually observed and coincided rather well with the light-off temperature for NO oxidation (see Fig. 1c and d). As seen in Fig. 4, addition of H_2 gave better activity for C_3H_6 conversion which is indicated by lower T_{50} values for both $NO/O_2/C_3H_6$ and $NO/O_2/CO/C_3H_6$ gas mixtures. Also, similar to Fig. 3b, addition of CO increased the light-off temperature for C_3H_6 both with and without H_2.

3.5. The effect of H_2 on N_2O formation and NO_x reduction

As addressed earlier, addition of H_2 with/without C_3H_6 may result in NO_x conversion over the Pt/Al_2O_3 catalyst. Fig. 5 displays the N balance and measured N_2O formation for the NO/O_2 and $NO/O_2/C_3H_6$ gas mixtures during the heating ramp. Formation of NH_3 was relatively low in all cases (below 10 ppm). As a result, the NH_3 concentration had a negligible effect on the *N* balance (Eq. (1)).

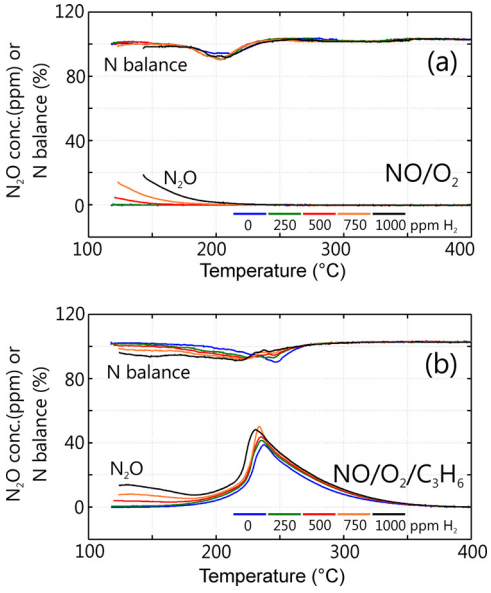

Fig. 5. The effect of H_2 on N_2O formation and N balance for NO/O_2 mixture (a) and $NO/O_2/C_3H_6$ mixture (b).

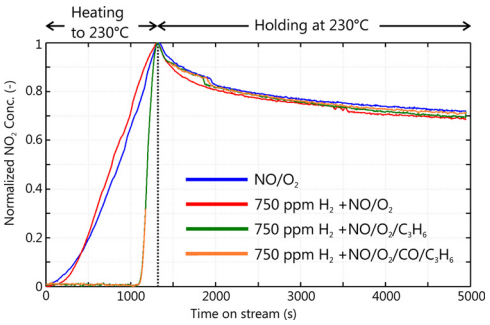

Fig. 6. The evolution of normalized NO_2 signal over various gas mixtures as a function of time under transient experimental mode 1.

As seen from Fig. 5a (NO/O_2), increasing H_2 concentration gave higher N_2O formation, notably in the low temperature region below 200 °C. In addition, the drop in the *N* balance as high as 10% was also found with a peak at 200 °C and it seems apparent that variation of the H_2 concentration did not affect neither the magnitude nor the temperature for the minimum *N* balance. As seen here, there was also a drop in the *N* balance even in the absence of H_2. Therefore, this consistent low temperature offset in the *N* balance was predominantly due to storage of nitrate species over the catalyst as in agreement with another study based on DRIFT analysis [25]. The results from the $NO/O_2/CO$ mixture (not shown) gave a similar N_2O formation and N balance profile as in Fig. 5a.

In the presence of C_3H_6, as for the $NO/O_2/C_3H_6$ gas mixture (Fig. 5b), formation of N_2O was more prominent and increased with higher H_2 concentration. The peak of N_2O in the range of 230–240 °C coincided rather well with the light-off for the NO oxidation reaction (Fig. 1c). The N balance drop of as much as 10%, in this case depended on the H_2 concentration and thus may result from a combination of both NO_x reduction and storage activities below 300 °C. It is worth noting that with a higher H_2 concentration, the drop of *N*-balance tended to decrease to lower temperatures. For the $NO/O_2/CO/C_3H_6$ mixture (not shown), similar results for the N_2O and NO_x conversion profiles as for the $NO/O_2/C_3H_6$ mixture were observed.

The overall results in Fig. 5 hence confirm the SCR activity as well as N_2O formation behavior as already reported in literature. The results that we obtained here confirm the higher selectivity for N_2O formation at low temperature with higher H_2 concentration as previously reported [10,26]. This can also be the reason for low NO_2 yield at low temperatures below 200 °C for the TPR data with NO/O_2 and $NO/O_2/CO$ mixtures, shown previously in Fig. 1a and b. The effect of H_2 on NO_x conversion/storage varied for different gas mixtures and the magnitude of N_2O formation is more pronounced for C_3H_6 containing mixtures. Since N_2O is known as a strong greenhouse gas, appreciable formation of N_2O due to addition of H_2 is indeed disadvantageous.

3.6. Transient NO_2 yields at constant temperature

As shown in [5], the NO_2 yield from NO oxidation reaction decreased as a function of time due to formation of Pt oxide. H_2 gave some promotional effect on NO_2 yield for all mixtures in the TPR experiments (Fig. 1) at about 230 °C. It was therefore of interest to investigate if H_2 may influence the decay in the NO oxidation activity due to Pt oxide formation at this temperature.

Fig. 6 presents the evolution of the normalized NO_2 signal for various gas mixtures as a function of time. The NO_2 signal was rescaled to within a range of 0–1 by normalization based on the maximum and minimum NO_2 outlet signals over the time range. It is worth noting that the results obtained during the heating ramp from 120 to 230 °C are consistent with the TPR data presented ear-

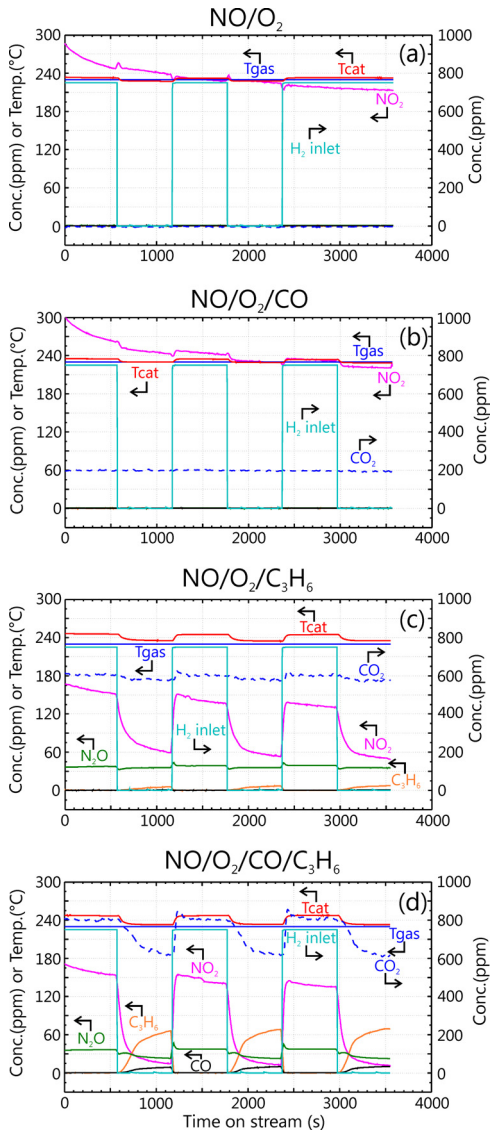

Fig. 7. The dynamic effects of switching in and out 750 ppm of H_2 with different gas mixtures (see Table 1). The catalyst was previously exposed to TPR by cofeeding 750 ppm of H_2 with corresponding gas mixture from 120 to 230 °C.

lier in Fig. 1. As seen from Fig. 6 when the temperature was held constant, there was a substantial decrease in the NO_2 signal as it dropped by as much as 30% from its maximum value. A comparison of the NO/O_2 mixture with the other H_2-containing gas mixtures, shows that the rate of decay of the NO_2 yields were similar. In fact, there was a slightly faster rate of decrease in NO_2 observed for NO/O_2 with H_2 compared to without H_2.

3.7. *Transient experiments with in/out H_2 switching*

To determine the dynamic effect of H_2 with various gas mixtures, transient experimental mode 2 was conducted and the results are presented in Fig. 7. Similar to Fig. 6, generally one can still observe a decline in the NO_2 signal as a function of time for all gas mixtures, despite the periodic switching of H_2. MS measurements indicated that H_2 was always fully converted in all cases. Introduction of 750 ppm of H_2, clearly caused the catalyst temperature (Tcat) to increase for all gas mixtures. In addition, the effect of H_2 on the N balance under these transient tests indicated that the effect of H_2 was small on the formation of N_2. The measured catalyst temperatures are also tabulated in Table 2. The temperature rise

Table 2
Catalyst temperatures during transient experiment during exposure of catalyst intermittently with 750 ppm H_2 with set point inlet gas temperature of 230 °C.

Gas mixtures	Approximate catalyst temperature (°C)	
	without H_2	with 750 ppm H_2
NO/O_2	227–228	232–233
$NO/O_2/CO$	228–230	234–235
$NO/O_2/C_3H_6$	235–237	245–246
$NO/O_2/CO/C_3H_6$	233	247–248

was naturally due to the exothermal H_2 combustion and was most prominently observed for the C_3H_6 containing mixtures. Therefore, the response of the NO_2 signal due to switching H_2 feed on and off, is due not only to possible effects of H_2 on surface chemistry and reactions but also to the temperature variations.

From Fig. 7a for the NO/O_2 mixture, it is apparent that switching H_2 in or out had little effect on the steady decline in NO_2 yield with time. Instead, feeding in H_2 generally caused a lower NO_2 yield which is contrary to the TPR results (Fig. 1a). From closer observation of the transient response at the start of the second cycle (at ca. 1200 s), it can be seen that the NO_2 signal first immediately dropped upon introduction of H_2 feed but then gradually recovered over a span of about 50 s.

The effect of H_2 on the $NO/O_2/CO$ mixture is shown in Fig. 7b. In contrast to the effect of H_2 on the NO/O_2 mixture, the effect of H_2 in this case was found to be positive by giving higher NO_2 yields in the presence of H_2. In addition, complete conversion of CO was always observed under these conditions as indicated by the CO_2 signal.

In the subsequent experimental sets, the effect of H_2 on C_3H_6 containing gas mixtures is shown in Fig. 7c and 7d. Addition of H_2 in these cases caused a notable increase not only in the NO_2 yield but also a slight increase in N_2O formation. It could also be seen that the effect of H_2 was almost instantaneous on NO_2 yield when switched in, however, when switched out it declined more slowly over about 5 min, nearly following the decline in the catalyst temperature. For the $NO/O_2/C_3H_6$ mixture (Fig. 7c), a remarkable increase in NO_2 yield from 60 ppm to ca. 150 ppm could be observed in the second H_2 switch cycle (at ca. 1200 s). Complete conversion of C_3H_6 was always observed in the presence of H_2, whereas in the absence of H_2, a small amount of C_3H_6 was detected in the outlet stream.

Similarly, the effect of H_2 to enhance NO_2 yield in $NO/O_2/CO/C_3H_6$ is clearly illustrated in Fig. 7d. Addition of H_2 in the second H_2 switch cycle (at ca. 1200 s) increased the NO_2 yield from 15 ppm to ca. 150 ppm. Again in the absence of H_2, C_3H_6 and CO concentrations were detected at 66 and 9 ppm, respectively. When H_2 was not fed, the NO_2 yield obtained for the $NO/O_2/CO/C_3H_6$ mixture was lower than that for $NO/O_2/C_3H_6$. Interestingly, the NO_2 yield obtained in the presence of H_2 was similar for both cases.

Fig. 8 shows the normalized NO_2 yields, H_2 feed and catalyst temperature from the second cycles in Fig. 7 (ca. 1200 s). Each of the values was rescaled in the range of 0–1 by normalization based on their maximum and minimum values within the time range. Thereby, this allowed the response times for the NO_2 yield and catalyst temperature to be more easily compared to probe the characteristics of the H_2 effect. It can be seen that the response in the NO_2 signal is faster than the temperature response. This is despite the fact that the response of NO_2 signal is subject to small measurement lag effects due to transport of gas from the monolith to the FTIR instrument and mixing effects in the analysis cell as has been scrutinized in [27]. Correction of the NO_2 response to offset these lag effects would only increase, although slightly, the faster response of NO_2 yield compared to temperature.

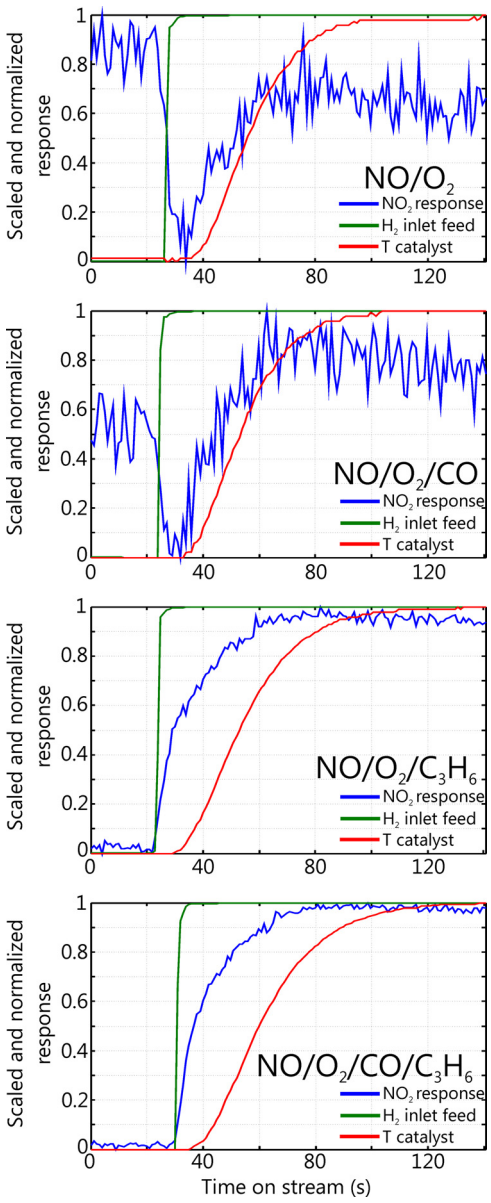

Fig. 8. The normalized NO_2, H_2 feed and catalyst temperature signals from the second cycles (ca. 1200 s) in Fig. 7 with corresponding gas mixtures.

For the NO/O_2 and $NO/O_2/CO$ mixtures, the NO_2 signal first decreased when H_2 feed started and then it increased at about the same rate as temperature began to increase. However, for both the $NO/O_2/C_3H_6$ and $NO/O_2/CO/C_3H_6$, the NO_2 signal immediately increased with H_2 feed and then continued to increase with the catalyst temperature. As presented in Table 2, the increase in the catalyst temperature was of course due to the exothermal heat from H_2 combustion. However it started to increase only about 15 s after the start of H_2 feed. This lag is partly due to the thermal inertia of the monolith catalyst and glass tube encasing the monolith. But also the time for axial heat conduction from the inlet where H_2 is mostly consumed to the outlet. Fig. 8 shows that in all cases, the heat of combustion of H_2 causes the NO_2 yield to increase. However the NO_2 signal also responded in different ways immediately following H_2 feed and this direct response should result from H_2 altering the surface species or reactions which in turn influences the NO_2 yield. In the case of the NO/O_2 and $NO/O_2/CO$ mixtures at these conditions, it is apparent that H_2 alters the surface reaction chemistry to have a negative influence on the NO_2 yield. In contrary for the $NO/O_2/C_3H_6$ and $NO/O_2/CO/C_3H_6$ mixtures, the H_2 effect on surface chemistry instead increases the NO_2 yield.

4. Discussion

4.1. Influence of H_2 on Pt oxide formation

It has been widely reported in literature that Pt oxide formation is the phenomena causing hysteresis behavior of NO oxidation over Pt/Al_2O_3 during heating/cooling ramps of TPR experiments. Hence, with the aid of Fig. 2 showing the hysteresis curves, one can observe that addition of H_2 modified the hysteresis behavior. This implies that H_2 likely plays a role to influence Pt oxide formation.

The extent of Pt oxide formation and the resulting hysteresis is reported to be related to the amount of NO_2 at medium and high temperatures near the thermodynamic equilibrium [8,9]. This is due to the strong oxidative power of NO_2 to promote Pt oxide formation [5]. To illustrate, for the NO/O_2 mixture cofeeding 1000 ppm of H_2 during heating ramp (see Fig 2a and e), resulted in higher NO_2 within the temperature interval 200–300 °C. This larger yield of NO_2 likely facilitated a greater formation of Pt oxide at the medium-high temperatures and this likely caused lower NO oxidation activity during the following cooling ramp. This resulted in the size of the hysteresis loop with 1000 ppm of H_2 being larger than in the absence of H_2. The results with varying H_2 concentration (250 to 750 ppm, not shown here) also indicated that increasing feed concentrations of H_2 broadened the size of the hysteresis loop for NO/O_2 mixtures.

For the $NO/O_2/CO/C_3H_6$ mixtures (Fig. 2d and 2 h), it is evident that the hysteresis loop here was smaller than that for the NO/O_2, which can be due to the role of C_3H_6 and H_2 to inhibit Pt oxidation. As displayed in the TPR data in Fig. 1d, increasing H_2 concentration beyond 500 ppm of H_2 clearly decreased the NO_2 yield within the medium-high temperature range. As a result, the lower NO_2 yield may reduce the extent of Pt oxide formation which results in a smaller gap between heating and cooling ramps in the presence of 1000 ppm of H_2.

As seen from Fig. 1a for the NO/O_2 mixture, addition of H_2 improved the NO_2 yield in temperature range of 200–300 °C. Improvement of NO_2 yield can be associated with H_2 preventing formation of inactive Pt oxide over the catalyst. Deactivation due to Pt oxide formation is obviously a slow process, occurring on the scale of several minutes as illustrated by Fig. 6. Also, at least at 230 °C, it occurs for all of the gas mixtures with or without H_2. It is likely then that H_2 hinders Pt oxide formation during the TPR, only at low temperatures, mostly below 200 °C, when H_2 conversion was less than complete. However, at temperatures above 200 °C, Pt oxide starts to form towards the rear part of the monolith which is no longer exposed to H_2, but is required for NO oxidation. The result is that the promotion of NO_2 formation with H_2 during the TPR with the NO/O_2 mixture was a temporary effect. It results from H_2 retarding Pt oxide formation at low temperature and the rate of Pt oxide formation lagging behind that of the temperature increase. As illustrated by Fig. 6 and 7a, when the temperature ramp was stopped at 230 °C, the Pt oxide formation was able to catch up and overtake the effect of the temperature increase. For operation at 230 °C (Fig. 7a), there was no longer any benefit remaining from any earlier retardation of Pt oxide formation. The transient experiment with NO/O_2 shown in Fig. 8 also demonstrated that switching in H_2 (2nd cycle at ca. 1200 s in Fig. 7a) gave an immediate decrease in NO_2 yield which was probably due to H_2 reacting with NO_2 to form NO rather than N_2 which is facilitated by the catalyst.

It is interesting to note from Fig 3a that the presence of CO in the absence of H_2 generally gave higher NO_2 yield for NO/O_2 as also shown in [9]. Similar to H_2, this enhancement effect of CO on NO oxidation is presumably due to the role of CO to retard Pt oxidation

at low temperature below 135 °C when CO was still detectable in the outlet stream [9,28]. With the relatively low CO concentration used here (200 ppm), it appears from comparison of Fig. 2a and 2b that CO has only a weak inhibition effect on NO oxidation. When H_2 and CO coexist, it is apparent that both species share the same function to retard Pt oxide formation. As a result, addition of H_2 to the $NO/O_2/CO$ mixture (Fig. 1b) resulted in only a marginal increase in NO_2 yield between 180 and 300 °C. It is also apparent that the effect of H_2 or CO to enhance NO_2 yield was only a temporal effect during the TPR experiment.

The addition of H_2 at 230 °C, shown in Fig. 7b, had only a minor influence on the NO_2 yield. Here, a slow gradual build-up of Pt oxide leading to decaying NO oxidation activity was still observable. Instead, an immediate negative effect of H_2 on NO_2 yield was observed for the $NO/O_2/CO$ mixture (Fig. 8) which can be due to surface reaction between H_2 and NO_2. Despite this immediate decrease in NO_2 yield, there was still a slight net positive effect of H_2 addition (Fig. 7b), but it was apparently only related to the exothermal heat of H_2 combustion as the increase of NO_2 signal was in closer proximity to the temperature increase (Fig. 8).

4.2. H_2 influence on C_3H_6 and CO oxidation and interactions with NO oxidation

In C_3H_6 containing mixtures, it is evident that C_3H_6 has a strong inhibition effect on NO oxidation at low temperature, before the onset of C_3H_6 oxidation (Fig. 1c and d). Addition of H_2 was found to weaken the inhibition effect of C_3H_6 by lowering the light-off temperature for C_3H_6 oxidation (Fig. 4) which in turn promoted NO oxidation. It is also notable that C_3H_6 caused the light-off temperature for CO oxidation to increase by about 27 °C (based on catalyst temperatures when 50% CO conversion was achieved, from Fig. 1b and 1d). In contrast, the first detection of NO_2 formation was delayed by about 100 °C or until almost complete conversion of C_3H_6 was obtained. This demonstrates how C_3H_6 has a considerably larger inhibiting effect on NO oxidation than CO oxidation. As shown in Fig. 4, the effect of CO to inhibit C_3H_6 conversion through competitive adsorption was also small probably due to the low concentration of CO used here.

It has been suggested that C_3H_6 inhibits NO oxidation by reaction of C_3H_6 with NO_2 to form NO particularly at low temperatures [20,23] as illustrated in the reaction below:

$$C_3H_{6(g)} + 9NO_{2(g)} \rightarrow 3CO_{2(g)} + 3H_2O_{(g)} + 9NO_{(g)} \quad (2)$$

There is also the possibility that C_3H_6 preferentially adsorbs on sites and thus blocks both NO and CO oxidation. Undoubtedly both of these inhibition mechanisms play a role. However, considering that C_3H_6 has a much stronger inhibition effect on NO oxidation rather than on CO oxidation, the reaction of C_3H_6 with NO_2 into NO would probably appear to be the more prominent cause of C_3H_6 inhibition on NO oxidation.

From the transient experimental results with $NO/O_2/C_3H_6$ and $NO/O_2/CO/C_3H_6$ mixtures in Fig. 7 and 8, it appeared that the H_2 effect to improve NO_2 yield was instantaneous. The transient data also confirms that H_2 activates C_3H_6 oxidation and thereby promotes the NO oxidation reaction. Interestingly, the increase in NO_2 signals were found to be faster than that of temperature, suggesting that H_2 affected adsorbed species and surface reactions in addition to the exothermal effect due to its combustion (Fig. 8). As addressed earlier, the effects of H_2 here can then be related to a decreased blocking effect of adsorbed C_3H_6 species and prevention of the reaction of C_3H_6 with NO_2 forming NO. It is also interesting to note that the NO_2 yield in Fig. 7c and 7d in the presence of H_2 were similar, which again confirms that H_2 facilitated complete oxidation of both C_3H_6 and CO to eliminate their inhibiting effects.

As shown by Hauff et al. [9], the presence of 2500 ppm of CO inhibits the NO oxidation reaction over Pt/Al_2O_3 at low temperature below the temperature for complete conversion of CO oxidation. This is due to self-inhibition of CO to block the Pt surface. The inhibition effect of CO on NO oxidation cannot be fully demonstrated in Fig. 1b probably due to the relatively low amount of CO used here (200 ppm of CO). As shown in Fig. 1b, addition of H_2 promotes CO oxidation by lowering the temperature for complete conversion of CO. Therefore, H_2 should also be able to promote NO oxidation for a $NO/O_2/CO$ mixture by eliminating inhibition effects of CO. Although H_2 lowers the light-off temperature for CO oxidation, the activity for NO oxidation below 130 °C is negligible (Fig. 1a) which makes the effect of H_2 to enhance NO_2 yield in a $NO/O_2/CO$ mixture become less prominent.

The TPR results with $NO/O_2/CO/C_3H_6$ (Fig. 1d) showed that the addition of a low concentration of H_2 such as 250 ppm appeared to be beneficial for NO oxidation with respect to light-off temperature as well as NO_2 yield over the entire temperature range. Therefore, it can be suggested that the addition of about 250 ppm of H_2 is optimal to enhance NO_2 yield for this complete DOC gas mixture. Higher H_2 concentrations were however found to lower the NO_2 yield for the temperature range of 250–400 °C. The detrimental effect of increasing H_2 concentration at these higher temperatures was probably due to NO_2 consumption by H_2.

5. Conclusions

In the present work, an evaluation of the H_2 effect on NO oxidation over Pt/Al_2O_3 was conducted using 4 gas mixtures: NO/O_2, $NO/O_2/CO$, $NO/O_2/C_3H_6$ and $NO/O_2/CO/C_3H_6$. Formation of Pt oxide is known to deactivate NO oxidation which is a slow process occurring over the scale of several minutes. Our results from TPR with NO/O_2 and $NO/O_2/CO$ mixtures showed that H_2 promoted the NO_2 yield in the temperature range of 200–300 °C. H_2 was proposed to retard Pt oxide formation mainly at low temperatures (below ca. 200 °C) when H_2 conversion was not complete and a substantial part of the monolith was exposed to H_2. As a result of slower formation of Pt oxide, there was a temporal enhancement of NO_2 yield due to H_2 at higher temperatures. For steady operation at higher temperatures with complete conversion of H_2, Pt oxide formation was unaffected by H_2. At these conditions, H_2 could even have a net negative effect on NO_2 yield probably by reaction with NO_2.

In C_3H_6 containing mixtures, it was evident that the promotional role of H_2 was to weaken the inhibition effect of C_3H_6 by lowering the light-off temperature for C_3H_6 oxidation. CO was found to have a weak inhibition effect on C_3H_6 oxidation and consequently also on NO oxidation. The results from transient experiments at 230 °C clearly showed an increase in NO_2 yield in the presence of H_2. The time response of the increase in the NO_2 signal was faster than the increase in catalyst temperature which indicated that H_2 had an effect on the catalytic surface chemistry to promote NO oxidation. The effects of H_2 can be related to a decreased blocking effect of adsorbed C_3H_6 species and prevention of the reaction of C_3H_6 with NO_2 to form NO.

H_2 did promote the oxidation of CO. However, CO was found to have only a weak inhibition effect on NO oxidation. As a result, at least for the CO feed concentration used here (200 ppm), H_2 did not promote NO oxidation by preventing CO inhibition. It appeared that CO also played a role to retard low temperature Pt oxide formation which gave higher NO_2 yield in the absence of H_2. Similar to the NO/O_2 mixture, a marginal temporal increase in NO_2 yield over the 200–300 °C temperature range was also obtained for H_2 addition to the $NO/O_2/CO$ mixture.

The TPR results with the $NO/O_2/CO/C_3H_6$ mixture showed that addition of a low concentration of H_2, such as 250 ppm, appeared to be beneficial for NO oxidation for nearly the entire temperature

range. It seems then probable that addition of about 250 ppm of H_2 is most optimal to enhance NO_2 yield for this complete DOC mixture. Higher H_2 concentrations tended to lower the NO_2 yield, probably due to NO_2 consumption by H_2 in the temperature range of 250–400 °C.

Acknowledgements

The financial support by the Swedish Research Council with grant number 621-2011-3926 is gratefully acknowledged. This work was performed within the Competence Centre for Catalysis, which is hosted by Chalmers University of Technology and financially supported by the Swedish Energy Agency and the member companies AB Volvo, ECAPS AB, Haldor Topsøe A/S, Scania CV AB, Volvo Car Corporation AB and Wärtsilä Finland Oy.

References

[1] A. Russell, W.S. Epling, Catal. Rev. 53 (2011) 337–423.
[2] L. Olsson, B. Westerberg, H. Persson, E. Fridell, M. Skoglundh, B. Andersson, J. Phys. Chem. B 103 (1999) 10433–10439.
[3] S.S. Mulla, N. Chen, W.N. Delgass, W.S. Epling, F.H. Ribeiro, Catal. Lett. 100 (2005) 267–270.
[4] D. Bhatia, R.W. McCabe, M.P. Harold, V. Balakotaiah, J. Catal. 266 (2009) 106–119.
[5] L. Olsson, E. Fridell, J. Catal. 210 (2002) 340–353.
[6] K. Hauff, H. Dubbe, U. Tuttlies, G. Eigenberger, U. Nieken, Appl. Catal. B- Environ. 129 (2013) 273–281.
[7] X. Auvray, T. Pingel, E. Olsson, L. Olsson, Appl. Catal. B- Environ. 129 (2013) 517–527.
[8] W. Hauptmann, M. Votsmeier, J. Gieshoff, A. Drochner, H. Vogel, Appl. Catal. B- Environ. 93 (2009) 22–29.
[9] K. Hauff, U. Tuttlies, G. Eigenberger, U. Nieken, Appl. Catal. B- Environ. 123–124 (2012) 107–116.
[10] J.M. Herreros, S.S. Gill, I. Lefort, A. Tsolakis, P. Millington, E. Moss, Appl. Catal. B- Environ. 147 (2014) 835–841.
[11] H. Hamada, M. Haneda, Appl. Catal. A- Gen. 421–422 (2012) 1–13.
[12] A. K.-i. Shimizu, Satsuma, Phys. Chem. Chem. Phys. 8 (2006) 2677–2695.
[13] M. Sun, E.B. Croiset, R.R. Hudgins, P.L. Silveston, M. Menzinger, Ind. Eng. Chem. Res. 42 (2002) 37–45.
[14] S. Salomons, M. Votsmeier, R.E. Hayes, A. Drochner, H. Vogel, J. Gieshof, Catal. Today 117 (2006) 491–497.
[15] S.R. Katare, P.M. Laing, SAE Int. J Fuels Lubr. 2 (2009-01-1268) (2015) 605–611.
[16] S. Salomons, R.E. Hayes, M. Votsmeier, Appl. Catal. A- Gen. 352 (2009) 27–34.
[17] W. Hauptmann, M. Votsmeier, H. Vogel, D.G. Vlachos, Appl. Catal. A- Gen. 397 (2011) 174–182.
[18] N.D. Hoyle, P. Kumarasamy, V.A. Self, P.A. Sermon, M.S.W. Vong, Catal. Today 47 (1999) 45–49.
[19] N. Rankovic, A. Nicolle, D. Berthout, P. Da Costa, J. Phys. Chem. C 115 (2011) 20225–20236.
[20] K. Irani, W.S. Epling, R. Blint, Appl. Catal. B- Environ. 92 (2009) 422–428.
[21] H. Oh, J. Luo, W. Epling, Catal. Lett. 141 (2011) 1746–1751.
[22] I.V. Yentekakis, V. Tellou, G. Botzolaki, I.A. Rapakousios, Appl. Catal. B- Environ. 56 (2005) 229–239.
[23] M. Al-Harbi, R. Hayes, M. Votsmeier, W.S. Epling, Can. J. Chem. Eng. 90 (2012) 1527–1538.
[24] R. Lanza, E. Eriksson, L.J. Pettersson, Catal. Today 147 (2009) S279–S284.
[25] X. Auvray, L. Olsson, Appl. Catal. B- Environ. 168–169 (2015) 342–352.
[26] J.-I. Yang, H. Jung, Chem. Eng. J. 146 (2009) 11–15.
[27] S. Soltani, R. Andersson, B. Andersson, Chem. Eng. J. 264 (2015) 188–196.
[28] M. Irfan, J. Goo, S. Kim, Environmentalist 31 (2011) 4–10.